



# Prediction of solar cycle 25: applications and comparison

Valentina Penza<sup>1</sup> · Luca Bertello<sup>2</sup> · Matteo Cantoresi<sup>1</sup> · Serena Criscuoli<sup>2</sup> · Francesco Berrilli<sup>1</sup>

Received: 6 June 2023 / Accepted: 19 July 2023 / Published online: 29 July 2023  
© The Author(s) 2023

## Abstract

Solar activity affects the heliosphere in different ways. Variations in particles and radiation that impact the Earth's atmosphere, climate, and human activities often in disruptive ways. Consequently, the ability to forecast solar activity across different temporal scales is gaining increasing significance. In this study, we present predictions for solar cycle 25 of three solar activity indicators: the core-to-wing ratio of Mg II at 280 nm, the solar radio flux at 10.7 cm—widely recognized proxies for solar UV emission—and the total solar irradiance, a natural driver of Earth's climate. Our predictions show a very good agreement with measurements of these activity indicators acquired during the ascending phase of solar cycle 25, representing the most recent data available at the time of writing.

**Keywords** Sun: activity · Sun: solar cycle

## 1 Introduction

Solar variability refers to variations of solar radiations and particles emitted by the Sun. Solar variability occurs across all spatial, temporal, and wavelength scales, and it is constantly monitored because it has a significant impact on the

near-Earth space environment, as well as on the upper and lower terrestrial atmosphere (e.g., Bordi et al. 2015; Matthes et al. 2017; Bigazzi et al. 2020; Lockwood and Ball 2020; Usoskin et al. 2002; Berrilli et al. 2014; Fiandrini et al. 2021). The primary driver of solar variability is the solar magnetic field, so particular attention is paid to studying the characteristics of the 11-year cycle, which is the most prominent modulation of the magnetic field. During this cycle, the Sun's magnetic activity increases and weakens, leading to a reversal of the dominant polarities in the polar regions. As a result, the appearance of the solar surface changes, with an increasing fraction of area covered by bright (plages) and dark (sunspots) structures. These changes, in turn, modulate the solar irradiance, the radiative power per unit area received at the top of the Earth's atmosphere (Petrie et al. 2021). Variations in total solar irradiance (TSI—the irradiance integrated over the whole energy spectrum) due to magnetic activity result in an overall change of approximately 0.1% (e.g., Wilson 1978; Hudson 1988; Kopp et al. 2016). However, these changes are not uniform across all wavelengths (e.g., Marchenko et al. (2021); Thuillier et al. (2022); Criscuoli et al. (2021)), and in some spectral bands, such as ultraviolet (e.g., Lovric et al. 2017; Criscuoli et al. 2023; Berrilli et al. 2020) or radio flux (e.g., Dudok de Wit et al. 2014), they can be much larger. Understanding spectral solar irradiance (SSI—hereafter) variations in different spectral bands is essential as SSI variability produces distinct impacts on our environment. For instance, the

---

Valentina Penza, Luca Bertello, Matteo Cantoresi, Serena Criscuoli and Francesco Berrilli have contributed equally to this work.

---

This paper belongs to the Topical collection “Frontiers in Italian studies on Space Weather and Space Climate”, that includes papers written on the occasion of the Second National Congress of SWiCo, “Space Weather Italian Community”, held on February 9–11 2022 in Rome’ at ASI, “Agenzia Spaziale Italiana”.

---

✉ Valentina Penza  
valentina.penza@roma2.infn.it

Luca Bertello  
luca@nso.edu

Matteo Cantoresi  
matteo.cantoresi@libero.it

Serena Criscuoli  
scriscuo@nso.edu

Francesco Berrilli  
francesco.berrilli@roma2.infn.it

<sup>1</sup> Dipartimento di Fisica, Università di Roma Tor Vergata, Via della Ricerca Scientifica 1, Rome 00133, Italy

<sup>2</sup> National Solar Observatory, 3665 Discovery Dr., Boulder, CO 80303, USA

extreme-UV (EUV—hereafter) creates disturbances in the thermosphere (e.g., Briand et al. 2021) and ionosphere (e.g., Floyd et al. 2002) thus affecting satellite orbits and radio-communications; ultraviolet light affects the production of ozone in the Earth's stratosphere and mesosphere (e.g., Haigh 1994; Matthes et al. 2006) while longer wavelengths reach the Earth's surface, heating oceans and thus affecting global circulation patterns (Gray et al. 2010). Solar irradiance is among the most prominent natural forcing of the Earth's climate (e.g., Jungclaus et al. 2017; Jing et al. 2021).

Solar activity also modulates the occurrence and frequency of violent and explosive solar phenomena, such as flares and coronal mass ejections, which are of great concern to human activities and artificial satellites orbiting the Earth. The cycles of solar activity are different from each other, with modulations at secular time scales, including the existence of Grand Minima (e.g., Vecchio et al. 2019), such as the Maunder minimum during the years 1645–1715 Hathaway (2015), and Grand Maxima periods Usoskin et al. (2007). Given the significant impact of solar activity on human activities and artificial satellites, there is a considerable amount of studies concerning the prediction of solar behavior. A comprehensive review of various methods for predicting solar cycles can be found in Petrovay (2020), while Jiang et al. (2023) offers a comparison of several forecasts for solar cycle 25th (SC25 from here on).

Typically, forecasting models are used to predict solar activity indicators such as SunSpot Number (e.g., McIntosh et al. 2020; Singh et al. 2021a), magnetic flux (e.g., Cameron et al. 2016; Bhowmik and Nandy 2018; Upton and Hathaway 2018; Labonville et al. 2019), or geomagnetic indices (e.g., Singh et al. 2021a). Recently, Penza et al. (2021) proposed a new approach that allows to predict the area coverage of sunspots and plages. This approach offers an advantage, as these quantities can be used to forecast a range of other important activity indices for space weather and climate, including spectral and total solar irradiance variability. In this paper, we employ precisely such coverages to predict the variability during SC25 of three fundamental proxies of the solar magnetic activity: the Mg II index at 280 nm (e.g., Viereck et al. 2004; Criscuoli et al. 2023; Snow et al. 2019; Berrilli et al. 2020), which is a proxy for solar UV radiation, the solar radio flux at 10.7 cm (Tapping 2013; Dudok de Wit et al. 2014; Selhorst et al. 2014), which is a proxy for solar EUV radiation, and the TSI, which, as explained above, is a natural forcing of the Earth's climate (e.g., Mendoza 2005; Engels and van Geel 2012; Schmutz 2021).

## 2 Prediction of active region coverage over cycle 25

The procedure adopted in Penza et al. (2021) to predict SC25 activity consists mainly in two steps, here briefly summarized:

1. We describe each cycle through a parametric form (Volobuev 2009), initially depending on two parameters  $Td_k$ , related to the duration of the cycle, and  $Ts_k$ , related to its intensity:

$$x_k(t) = \left( \frac{t - T0_k}{Ts_k} \right)^2 e^{-\left( \frac{t - T0_k}{Td_k(Ts_k)} \right)^2} \quad \text{for } T0_k < t < T0_k + \tau_k, \quad (1)$$

where  $T0_k$  represents the start time of the  $k$ th cycle. The values of these parameters are obtained by fitting sunspot and plage composite data published in Mandal et al. (2020) and Chatzistergos et al. (2019), respectively, as available at the Max Planck Institute site<sup>1</sup> at the date of December 2021. Both datasets cover a time period from the end of the nineteenth century approximately to 2019.

It is possible to reduce the number of parameters from two to one, as  $Td_k$  and  $Ts_k$  are related to each other by the following:

$$\begin{aligned} Td_k^{\text{plage}} &= (0.09 \pm 0.01) Ts_k^{\text{plage}} + (3.27 \pm 0.10) \text{ yr} \\ Td_k^{\text{spot}} &= (0.022 \pm 0.001) Ts_k^{\text{spot}} + (2.98 \pm 0.04) \text{ yr}. \end{aligned} \quad (2)$$

The relations in Eq. 2 are consequence of a solar cycle behavior known in the literature as Waldmeier effect (e.g., Hathaway et al. 1994; Hazra et al. 2015): the stronger the cycle ( $Ts_k$  smaller), the shorter its duration ( $Td_k$ ).

The functional form that describes the shape of each cycle becomes monoparametric by replacing the  $Td_k$  values in Eq. 2 into Eq. 1.

2. We identify an odd–even relationship of the parameters  $Ts_{2k+1}$  versus  $Ts_{2k}$  for sunspot and plage coverage relations:

$$\begin{aligned} Ts_o^{\text{plage}} &= (0.74 \pm 0.08) Ts_e^{\text{plage}} + (1.5 \pm 1.1) \text{ yr} \\ Ts_o^{\text{spot}} &= (0.69 \pm 0.05) Ts_e^{\text{spot}} + (11 \pm 3) \text{ yr}, \end{aligned} \quad (3)$$

where the subscripts  $o$  and  $e$  denote odd and even, respectively. Equation 3 provides the two  $Ts$  parameters (one for plage, one for sunspots) that can be used to predict plage and sunspot area coverages during SC25. Both predictions are shown in Fig. 1, together with their uncertainties, whose derivation is explained in Penza et al. (2021).

<sup>1</sup> <http://www2.mps.mpg.de/projects/sun-climate/data.html>.

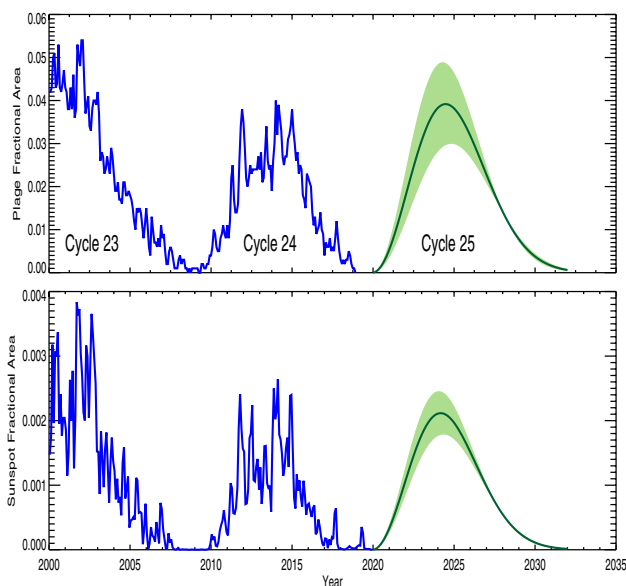
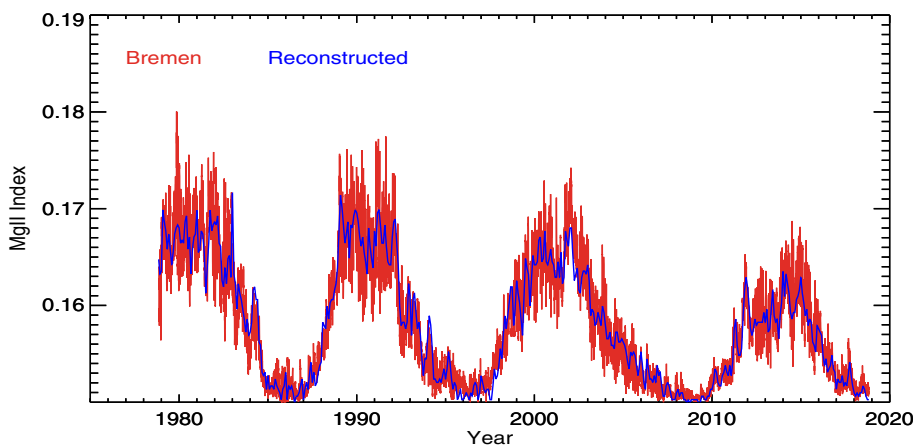


**Fig. 1** Prediction of plage coverage (top panel) and sunspot coverage (bottom panel). The shadow green area defines the lower and upper limits

### 3 Prediction of activity indices: Mg II and radio flux

We use the sunspot and plage area coverage predictions described above to predict two magnetic activity indicators: the core-to-wing ratio Mg II index at 280 nm and the Radio Flux at 10.7 cm.

**Fig. 2** Comparison between Mg II index reconstruction and Bremen data composite



The Mg II core-to-wing index is computed by using the definition given in Yeo et al. (2014):

$$\text{Mg II}(t) = 2 \frac{\int_{279}^{281} E(\lambda, t) d\lambda}{\int_{276}^{277} E(\lambda, t) d\lambda + \int_{284}^{283} E(\lambda, t) d\lambda}, \tag{4}$$

where  $E(\lambda, t)$  is the spectral irradiance at the time  $t$ . Assuming that variations of the Mg II index are modulated only by bright structures (Lean et al. 1997), we can rewrite Eq. 4 as:

$$\text{Mg II}(t) = 2 \frac{\alpha_f(t)I_f^{(\text{core})} + [1 - \alpha_f(t)]I_q^{(\text{core})}}{\alpha_f(t)I_f^{(\text{cont})} + [1 - \alpha_f(t)]I_q^{(\text{cont})}}, \tag{5}$$

where  $\alpha_f$  indicates the coverage fraction of faculae,  $I$  the integral of intensity, while the subscripts ( $f$ ) and ( $q$ ) indicate facular and quiet contributions, respectively. If we factor out the  $I_q$  terms, we obtain

$$\frac{\text{Mg II}(t)}{\text{Mg II}_q} = \frac{\alpha_f(t)\delta^{(\text{core})} + 1}{\alpha_f(t)\delta^{(\text{wing})} + 1}, \tag{6}$$

where  $\delta^{\text{core}}$  and  $\delta^{\text{wing}}$  are the relative contrasts of the intensity at the core and in the wings, respectively, between facular and quiet regions, and  $\text{Mg II}_q$  is the value of the index during a period of minimum. Following Penza et al. (2022), we treat  $\delta^{\text{core}}$  and  $\delta^{\text{wing}}$  as free parameters and derive them by fitting the  $\frac{\text{Mg II}(t)}{\text{Mg II}_q}$  expression with the Bremen Mg II composite

**Fig. 3** Prediction of the Mg II index for SC25 and Bremen data composite, smoothed using a gaussian kernel of one month. The shaded area represents uncertainties in the prediction

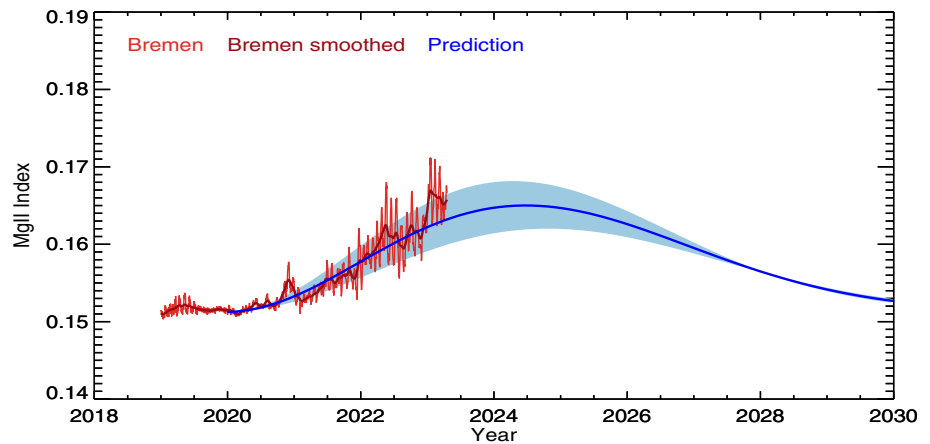
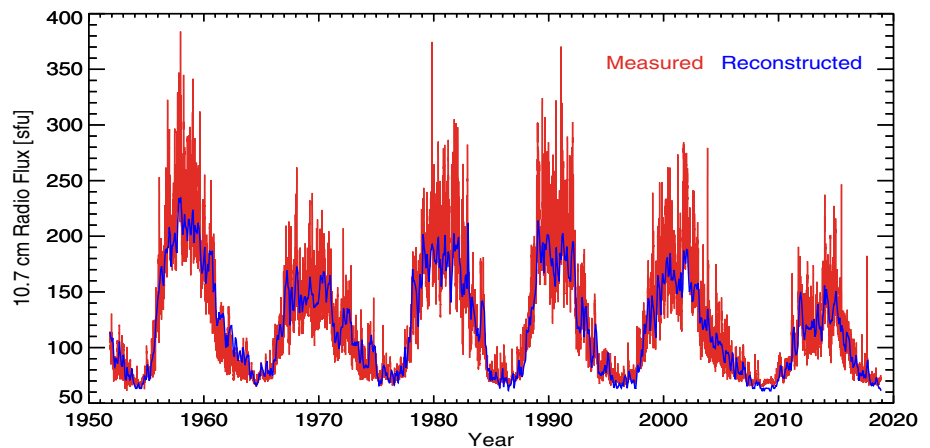


**Fig. 4** Comparison between radio flux reconstruction and CLS time series at 10.7 cm, smoothed using a gaussian kernel of one month



data.<sup>2</sup> By choosing  $Mg\ II_q = 0.1499$ , which is the Mg II index value at the minimum between the 21st and the 22nd cycles, we find  $\delta^{(core)} = 3.708 \pm 0.007$  and  $\delta^{(wing)} = 1.312 \pm 0.006$ . These values are in a reasonable agreement with wing and core contrast values obtained with spectral syntheses (Fontenla et al. 2011; Criscuoli et al. 2023). The contrast value found for faculae is actually slightly higher, as a result of our model not distinguishing between facular and network contributions.

The Mg II index reconstructed using the fit in Eq. 6 is shown in Fig. 2, while the prediction, obtained combining the fitted contrast values with the predicted area coverage of faculae, is shown in Fig. 3. The prediction is also compared with the Bremen Mg II index measured during the ascending phase of SC25. The shaded area represents uncertainties in the prediction obtained by propagating the error relative to the alone coverage  $\alpha_f$ , the error of the contrast coefficients being much smaller. This is the case also for the following

reconstructions. The plot shows a very good agreement between our forecast and the measurements.

Using a similar approach, we can reconstruct and predict the solar radio flux at 10.7 cm  $F^{10.7}$ . In this case, the parametric expression is:

$$\frac{F^{(10.7)}(t)}{F_q^{(10.7)}} = [\alpha_f(t) + \alpha_s(t)]\delta^{(10.7)} + 1, \quad (7)$$

where  $F_q^{(10.7)}$  is the radio flux measured at a period of minimum. Unlike in the case of the Mg II index, for the radio emission we have taken into account the contribution of both faculae and sunspots (whose area coverages are represented by  $\alpha_f$  and  $\alpha_s$ , respectively), and their contrast is modeled using a single parameter  $\delta^{10.7}$  as both features contribute positively. That is because the emission at 10.7 cm arises mainly from strong magnetic field regions in the chromosphere and transition region, morphologically associated with the plage, but also from sunspots (e.g., Foukal 1998;

<sup>2</sup> Available at [https://lasp.colorado.edu/lisird/data/bremen\\_composite\\_MgII/](https://lasp.colorado.edu/lisird/data/bremen_composite_MgII/).

**Fig. 5** Prediction of the solar radio flux at 10.7 cm for solar cycle 25 and CLS time series at 10.7 cm, smoothed using a gaussian kernel of one month bandwidth

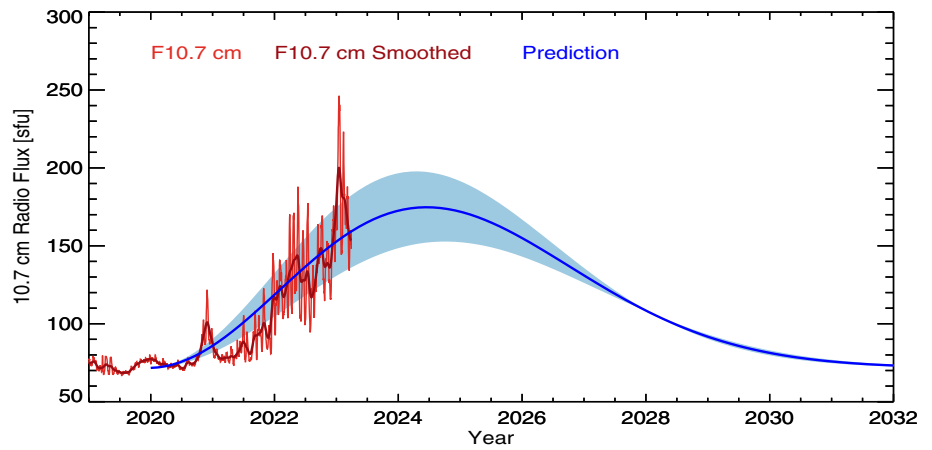


**Fig. 6** Comparison between TSI reconstruction and PMOD composite

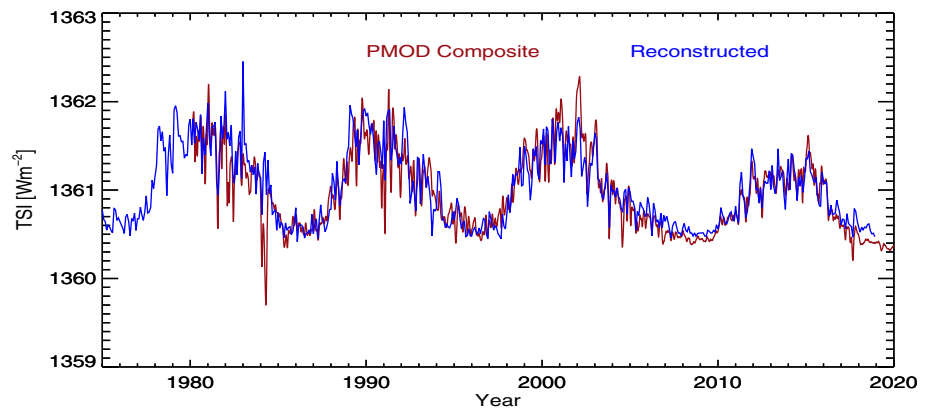
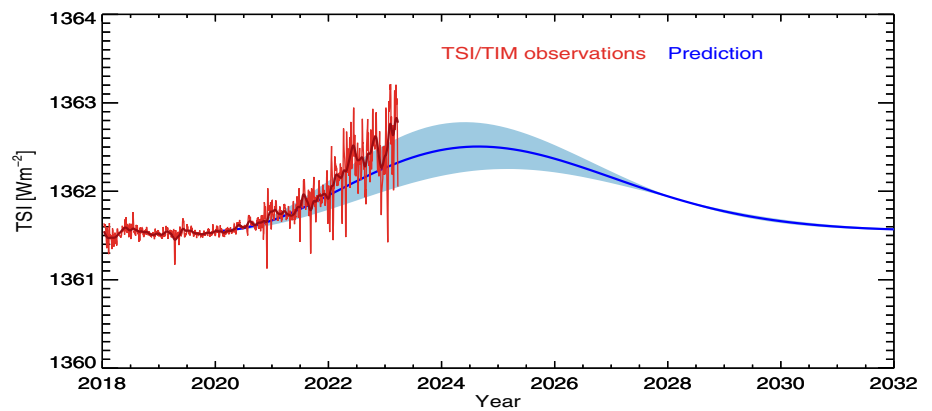


**Fig. 7** Prediction of the TSI for solar cycle 25. The predicted irradiance values were increased by 1.07 W/m<sup>2</sup> to reconcile them with TSIS/TIM measurements



Tapping 1987; Bastian et al. 1996; Schmahl and Kund 1995; Singh et al. 2021b).

The value of the  $\delta^{10.7}$  parameter is obtained by fitting Eq. 7 with the CLS Solar Radio Flux at 10.7 cm time series.<sup>3</sup> By using  $F_q^{(10.7)} = 64.1$  (solar flux unit), which is the value of the radio flux at the minimum between the 18th and 19th

cycle, we find  $\delta^{(10.7\text{ cm})} = 36.37 \pm 0.01$ . The reconstructed and predicted  $F^{10.7}$  values are shown in Figs. 4 and 5, respectively. Even for the radio flux we find that our prediction agrees with measurements obtained during the rising phase of SC25 within the uncertainties of the model.

<sup>3</sup> Available at [https://lasp.colorado.edu/lisird/data/cls\\_radio\\_flux\\_f107](https://lasp.colorado.edu/lisird/data/cls_radio_flux_f107).

## 4 Prediction of TSI

The TSI along the 25th cycle is predicted by using the equation and the parameters derived by Penza et al. (2022):

$$\Delta F(t) = C_n + \alpha_f(t)\delta_{fn}^{(TSI)} + \alpha_s(t)\delta_s^{(TSI)}, \quad (8)$$

where  $C_n$  is a constant and represents the product between the network contrast and the network coverage when the facular coverage is zero,  $\delta_{fn}^{(TSI)}$  is a linear combination of network and facular relative contrast, while  $\delta_s^{(TSI)}$  is the sunspot relative contrast. The values for the three parameters found in Penza et al. (2022) by fitting Eq. 8 with the PMOD TSI composite<sup>4</sup> are:  $C_n = 1.31 \times 10^{-3} \pm 6 \times 10^{-5}$ ,  $\delta_{fn}^{(TSI)} = 0.027 \pm 0.004$  and  $\delta_s^{(TSI)} = -0.17 \pm 0.06$ . The corresponding TSI reconstruction and prediction are reported in Figs. 6 and 7, respectively. The TSI prediction is compared to TSIS/TIM observations.<sup>5</sup> The agreement is rather good, after correcting the prediction by  $1.07 \text{ W/m}^2$ , as expected from the analysis presented in Montillet et al. (2022).

## 5 Conclusions

In this work, we have presented a method to predict solar activity indices such as the Mg II core-to-wing ratio at 280 nm, the radio Flux at 10.7, and total solar irradiance for SC25. The method is obtained from the forecast of sunspot and plage areas described in Penza et al. (2021). The adopted approach is parametric, which makes possible to reconstruct magnetic activity indicators and solar irradiance for past epochs as well as to make future predictions. The procedure is based on an empirically derived relation (Eq. 3) between the strength of *odd* and *even* cycles, which is in agreement with the Gnevyshev–Ohl rule (Gnevyshev and Ohl 1948) stating that the strength of an even cycle is lower than the strength of the subsequent odd cycle.

We have compared our forecasts with observations acquired during the rising phase of SC25, which are the latest observations available at the time of the writing of this paper. We have found that our predictions present in general a very good agreement with the observations. The TSI is slightly underestimated. This could indicate that the sunspot prediction is slightly overestimated and/or that the different dataset used for comparison (TSIS/TIM instead PMOD composite) would have required a slightly different value of  $\delta_s$  value.

<sup>4</sup> Available at <ftp.pmodwrc.ch/pub/data/irradiance/virgo/TSI/TSI-composite/>.

<sup>5</sup> Available at <https://lasp.colorado.edu/lisird/>.

**Acknowledgements** The authors thank Dr Angela Cookson for useful discussions. The National Solar Observatory is operated by the Association of Universities for Research in Astronomy, Inc. (AURA), under cooperative agreement with the National Science Foundation. M. Cantoresi is supported by the Joint Research PhD Program in “Astronomy, Astrophysics and Space Science” between the universities of Roma Tor Vergata and Roma Sapienza, and INAF.

**Author Contributions** Not applicable.

**Funding** Open access funding provided by Università degli Studi di Roma Tor Vergata within the CRUI-CARE Agreement. Not applicable.

**Data availability statement** Not applicable.

## Declarations

**Conflict of interest** Not applicable

**Ethics approval** Not applicable.

**Consent to participate** Not applicable.

**Consent for publication** Not applicable.

**Code availability** Not applicable.

**Open Access** This article is licensed under a Creative Commons Attribution 4.0 International License, which permits use, sharing, adaptation, distribution and reproduction in any medium or format, as long as you give appropriate credit to the original author(s) and the source, provide a link to the Creative Commons licence, and indicate if changes were made. The images or other third party material in this article are included in the article’s Creative Commons licence, unless indicated otherwise in a credit line to the material. If material is not included in the article’s Creative Commons licence and your intended use is not permitted by statutory regulation or exceeds the permitted use, you will need to obtain permission directly from the copyright holder. To view a copy of this licence, visit <http://creativecommons.org/licenses/by/4.0/>.

## References

- Bastian TG, Dulk G, Leblanc Y (1996) High resolution microwave observations of the quiet solar chromosphere. *ApJ* 473:539. <https://doi.org/10.1086/178165>
- Berrilli F, Casolino M, Del Moro D, Di Fino L, Larosa M, Narici L, Piazzesi R, Picozza P, Scardigli S, Sparvoli R, Stangalini M, Zacontè V (2014) The relativistic solar particle event of May 17th, 2012 observed on board the International Space Station. *J Space Weather Space Climate* 4:16. <https://doi.org/10.1051/swsc/2014014>
- Berrilli F, Criscuoli S, Penza V, Lovric M (2020) Long-term (1749–2015) variations of solar UV spectral indices. *Sol Phys* 295(3):38. <https://doi.org/10.1007/s11207-020-01603-5>
- Bhowmik P, Nandy D (2018) Prediction of the strength and timing of sunspot cycle 25 reveal decadal-scale space environmental conditions. *Nat Commun* 9:5209. <https://doi.org/10.1038/s41467-018-07690-0>
- Bigazzi A, Cauli C, Berrilli F (2020) Lower-thermosphere response to solar activity: an empirical-mode-decomposition analysis of GOCE 2009–2012 data. *Ann Geophys* 38(3):789–800. <https://doi.org/10.5194/angeo-38-789-2020>

- Bordi I, Berrilli F, Pietropaolo E (2015) Long-term response of stratospheric ozone and temperature to solar variability. *Ann Geophys* 33(3):267–277. <https://doi.org/10.5194/angeo-33-267-2015>
- Briand C, Doerksen K, Deleflie F (2021) Solar EUV-enhancement and thermospheric disturbances. *Space Weather* 19(12):02840. <https://doi.org/10.1029/2021SW002840>
- Cameron RH, Jiang J, Schüssler M (2016) Solar cycle 25: another moderate cycle? *ApJ* 823(2):22. [arXiv:1604.05405](https://arxiv.org/abs/1604.05405) [astro-ph.SR]. <https://doi.org/10.3847/2041-8205/823/2/L22>
- Chatzistergos T, Ermolli I, Krivova NA, Solanki SK (2019) Analysis of full disc Ca II K spectroheliograms II. Towards an accurate assessment of long-term variations in plage areas. *A & A* 625:22. <https://doi.org/10.1051/0004-6361/201834402>
- Criscuoli S, Marchenko S, DeLand MT, Choudhary DP, Kopp G (2021) Solar activity and responses observed in Balmer lines. *A & A* 646:81. <https://doi.org/10.1051/0004-6361/202037767>
- Criscuoli S, Penza V, Lovric M, Berrilli F (2023) Understanding Sun-as-a-star variability of solar Balmer lines. *ApJ*. [arXiv:2305.05510](https://arxiv.org/abs/2305.05510) [astro-ph.SR]
- Dudok de Wit T, Bruinsma S, Shibasaki K (2014) Synoptic radio observations as proxies for upper atmosphere modelling. *J Space Weather Space Climate* 4:A06
- Engels S, van Geel B (2012) The effects of changing solar activity on climate: contributions from palaeoclimatological studies. *J Space Weather Space Climate* 2:09. <https://doi.org/10.1051/swsc/201209>
- Fiandrini E, Tomassetti N, Bertucci B, Donnini F, Graziani M, Khiali B, Reina Conde A (2021) Numerical modeling of cosmic rays in the heliosphere: analysis of proton data from AMS-02 and PAMELA. *Phys Rev D* 104(2):023012. [arXiv:2010.08649](https://arxiv.org/abs/2010.08649) [astro-ph.HE]. <https://doi.org/10.1103/PhysRevD.104.023012>
- Floyd L, Tobiska WK, Cebula RP (2002) Solar UV irradiance, its variations, and its relevance to the earth. *Adv Space Res* 29(10):1427–14402. [https://doi.org/10.1016/S0273-1177\(02\)00202-8](https://doi.org/10.1016/S0273-1177(02)00202-8)
- Fontenla JM, Harder J, Livingston W, Snow M, Woods T (2011) High-resolution solar spectral irradiance from extreme ultraviolet to far infrared. *J Geophys Res (Atmospheres)* 116:20108. <https://doi.org/10.1029/2011JD016032>
- Foukal P (1998) Extension of the F10.7 index to 1905 using Mt. Wilson Ca K spectroheliograms. *Geophys Res Lett* 25(15):2909. <https://doi.org/10.1029/98GL02057>
- Gnevyshevi MN, Ohl AI (1948) On 22 year cycle of the solar activity. *Astron Zh* 25:18–20
- Gray LJ, Beer J, Geller M, Haigh JD, Lockwood M, Matthes K, Cubasch U, Fleitmann D, Harrison G, Hood L, Luterbacher J, Meehl GA, Shindell D, van Geel B, White W (2010) Solar influences on climate. *Rev Geophys* 48(4):4001. <https://doi.org/10.1029/2009RG000282>
- Haigh JD (1994) The role of stratospheric ozone in modulating the solar radiative forcing of climate. *Nature* 370(6490):544–546. <https://doi.org/10.1038/370544a0>
- Hathaway DH (2015) The solar cycle. *Living Rev Sol Phys* 12:87. <https://doi.org/10.1007/lrsp-2015-4>
- Hathaway DH, Hathaway DH, Reichmann J (1994) The shape of the sunspot cycle. *Sol Phys* 151:177–190. <https://doi.org/10.1007/BF00654090>
- Hazra G, Karak BB, Banerjee D, Choudhuri AR (2015) Correlation between decay rate and amplitude of solar cycles as revealed from observations and dynamo theory. *Sol Phys* 290(6):1851–1870. [arXiv:1410.8641](https://arxiv.org/abs/1410.8641) [astro-ph.SR]. <https://doi.org/10.1007/s11207-015-0718-8>
- Hudson HS (1988) Observed variability of the solar luminosity. *ARA & A* 26:473–507. <https://doi.org/10.1146/annurev.aa.26.090188.002353>
- Jiang J, Zhang Z, Petrovay K (2023) Comparison of physics-based prediction models of solar cycle 25. *J Atmos Sol Terr Phys* 243:106018
- Jing X, Huang X, Chen X, Wu DL, Pilewskie P, Coddington O, Richard E (2021) Direct influence of solar spectral irradiance on the high-latitude surface climate. *J Climate* 34(10):4145–4158. <https://doi.org/10.1175/JCLI-D-20-0743.1>
- Jungclauss JH, Bard E, Baroni M, Braconnot P, Cao J, Chini LP, Egorova T, Evans M, Fidel González-Rouco J, Goosse H, Hurtt GC, Joos F, Kaplan JO, Khodri M, Klein Goldewijk K, Krivova N, LeGrande AN, Lorenz SJ, Luterbacher J, Man W, Maycock AC, Meinshausen M, Moberg A, Muscheler R, Nehrbass-Ahles C, Otto-Bliesner BI, Phipps SJ, Pongratz J, Rozanov E, Schmidt GA, Schmidt H, Schmutz W, Schurer A, Shapiro AI, Sigl M, Smerdon JE, Solanki SK, Timmreck C, Toohey M, Usoskin IG, Wagner S, Wu C-J, Leng Yeo K, Zanchettin D, Zhang Q, Zorita E (2017) The PMIP4 contribution to CMIP6—part 3: the last millennium, scientific objective, and experimental design for the PMIP4 past1000 simulations. *Geosci Model Dev* 10(11):4005–4033. <https://doi.org/10.5194/gmd-10-4005-2017>
- Kopp G, Krivova N, Wu CJ, Lean J (2016) The impact of the revised sunspot record on solar irradiance reconstructions. *Sol Phys* 291:2951–2965. [arXiv:1601.05397](https://arxiv.org/abs/1601.05397) [astro-ph.SR]. <https://doi.org/10.1007/s11207-016-0853-x>
- Labonville F, Charbonneau P, Lemerle A (2019) A dynamo-based forecast of solar cycle 25. *Sol Phys* 294:82. <https://doi.org/10.1007/s11207-019-1480-0>
- Lean JL, Rottman GJ, Kyle HL, Woods TN, Hickey JR, Puga LC (1997) Detection and parameterization of variations in solar mid- and near-ultraviolet radiation (200–400 nm). *J Geophys Res* 102(D25):29939–29956. <https://doi.org/10.1029/97JD02092>
- Lockwood M, Ball WT (2020) Placing limits on long-term variations in quiet-Sun irradiance and their contribution to total solar irradiance and solar radiative forcing of climate. *Proc R Soc A*. <https://doi.org/10.1098/rspa.2020.0077>
- Lovric M, Tosone F, Pietropaolo E, Del Moro D, Giovannelli L, Cagnazzo C, Berrilli F (2017) The dependence of the [FUV-MUV] colour on solar cycle. *J Space Weather Space Climate* 7(27):6. [arXiv:1606.08267](https://arxiv.org/abs/1606.08267) [astro-ph.SR]. <https://doi.org/10.1051/swsc/2017001>
- Mandal S, Krivova NA, Solanki SK, Sinha N, Banerjee D (2020) Sunspot area catalog revisited: daily cross-calibrated areas since 1874. *A & A* 640:78. [arXiv:2004.14618](https://arxiv.org/abs/2004.14618) [astro-ph.SR]. <https://doi.org/10.1051/0004-6361/202037547>
- Marchenko S, Criscuoli S, DeLand MT, Choudhary DP, Kopp G (2021) Solar activity and responses observed in Balmer lines. *A & A* 646:81. <https://doi.org/10.1051/0004-6361/202037767>
- Matthes K, Kuroda Y, Kodera K, Langematz U (2006) Transfer of the solar signal from the stratosphere to the troposphere: Northern winter. *J Geophys Res (Atmospheres)* 111(D6):06108. <https://doi.org/10.1029/2005JD006283>
- Matthes K, Funke B, Andersson ME, Barnard L, Beer J, Charbonneau P, Clilverd MA, Dudok de Wit T, Haberleiter M, Hendry A, Jackman CH, Kretschmar M, Kruschke T, Kunze M, Langematz U, Marsh DR, Maycock AC, Misios S, Rodger CJ, Scaife AA, Seppälä A, Shangguan M, Sinnhuber M, Tourpali K, Usoskin I, van de Kamp M, Veronen PT, Versick S (2017) Solar forcing for CMIP6 (v3.2). *Geosci Model Dev* 10:2247–2302. <https://doi.org/10.5194/gmd-10-2247-2017>
- McIntosh SW, Chapman S, Leamon RJ, Egeland R, Watkins NW (2020) Overlapping magnetic activity cycles and the sunspot number: forecasting sunspot cycle 25 amplitude. *Sol Phys* 295(12):163. [arXiv:2006.15263](https://arxiv.org/abs/2006.15263) [astro-ph.SR]. <https://doi.org/10.1007/s11207-020-01723-y>
- Mendoza B (2005) Total solar irradiance and climate. *Adv Space Res* 35(5):882–890. <https://doi.org/10.1016/j.asr.2004.10.011>

- Montillet J-P, Finsterle W, Kermarrec G, Sikonja R, Haberreiter M, Schmutz W, Dudok de Wit T (2022) Data fusion of total solar irradiance composite time series using 41 years of satellite measurements. *J Geophys Res (Atmospheres)* 127(13):2021–036146. <https://doi.org/10.1029/2021JD036146>
- Penza V, Berrilli F, Bertello L, Cantoresi M, Criscuoli S (2021) Prediction of sunspot and plage coverage for solar cycle 25. *ApJ* 922:12. <https://doi.org/10.3847/2041-8213/ac3663>
- Penza V, Berrilli F, Bertello L, Cantoresi M, Criscuoli S, Giobbi G (2022) Total solar irradiance during the last five centuries. *ApJ* 937:84. <https://doi.org/10.3847/1538-4357/ac8a4b>
- Petrie G, Criscuoli S, Bertello L (2021) Solar magnetism and radiation. In: Raouafi NE, Vourlidis A (eds) *Solar Physics and Solar Wind*, vol 1, p 83. <https://doi.org/10.1002/9781119815600.ch3>
- Petrovay K (2020) Solar cycle prediction. *Living Rev Sol Phys* 17:2. <https://doi.org/10.1007/s41116-020-0022-z>
- Schmahl E, Kund M (1995) Microwave proxies for sunspot blocking and total irradiance. *J Geophys Res.* <https://doi.org/10.1029/95JA00677>
- Schmutz WK (2021) Changes in the total solar irradiance and climatic effects. *J Space Weather Space Climate* 11:40. <https://doi.org/10.1051/swsc/2021016>
- Selhorst CL, Costa JE, de Castro CGG, Valio A, Pacini AA, Shibasaki K (2014) The 17 GHz active region number. *ApJ* 790:134. <https://doi.org/10.1088/0004-637X/790/2/134>
- Singh PR, Saad Farid A, Singh A, Pant TK, Aly AA (2021) Predicting the maximum sunspot number and the associated geomagnetic activity indices  $a_a$  and  $A_p$  for solar cycle 25. *Astrophys Space Sci* 366:48. <https://doi.org/10.1007/s10509-021-03953-3>
- Singh VK, Chandra S, Thomas S, Sharma SK, Vats HO (2021) A long-term multifrequency study of solar rotation using the solar radio flux and its relationship with solar cycles. *Mon Not R Astron Soc* 505:5228. <https://doi.org/10.1093/mnras/stab1574>
- Snow M, Machol J, Viereck R, Woods T, Weber M, Woodraska D, Elliott J (2019) A revised magnesium II core-to-wing ratio from solar solstice. *Earth Space Sci* 6(11):2106–2114. <https://doi.org/10.1029/2019EA000652>
- Tapping K (1987) Recent solar radio astronomy at centimeter wavelengths: the temporal variability of the 10.7 cm flux. *J. Geophysics Res* 92:829
- Tapping KF (2013) The 10.7 cm solar radio flux ( $F_{10.7}$ ). *Space Weather* 11(7):394–406. <https://doi.org/10.1002/swe.20064>
- Thuillier G, Zhu P, Snow M, Zhang P, Ye X (2022) Characteristics of solar-irradiance spectra from measurements, modeling, and theoretical approach. *Light Sci Appl* 11(1):79. <https://doi.org/10.1038/s41377-022-00750-7>
- Upton LA, Hathaway DH (2018) An updated solar cycle 25 prediction with AFT: the modern minimum. *Geophys Res Lett* 45(16):8091–8095. [arXiv:1808.04868 \[astro-ph.SR\]. https://doi.org/10.1029/2018GL078387](https://doi.org/10.1029/2018GL078387)
- Usoskin IG, Solanki SK, Kovaltsov GA (2007) Grand minima and maxima of solar activity: new observational constraints. *Å* 471:301–309. <https://doi.org/10.1051/0004-6361:20077704>
- Usoskin IG, Mursula K, Solanki SK, Schüssler M, Kovaltsov GA (2002) A physical reconstruction of cosmic ray intensity since 1610. *J Geophys Res (Space Physics)* 107(A11):1374. <https://doi.org/10.1029/2002JA009343>
- Vecchio A, Lepreti F, Laurenza M, Carbone V, Alberti T (2019) Solar activity cycles and grand minima occurrence. *Nuovo Cimento C Geophys Space Phys C* 42(1):15. <https://doi.org/10.1393/ncc/i2019-19015-0>
- Viereck RA, Floyd LE, Crane PC, Woods TN, Knapp BG, Rottman G, Weber M, Puga LC, DeLand MT (2004) A composite Mg II index spanning from 1978 to 2003. *Space Weather* 2:10005. <https://doi.org/10.1029/2004SW000084>
- Volobuev DM (2009) The shape of the sunspot cycle: a one-parameter fit. *Sol Phys* 258:319–330. <https://doi.org/10.1007/s11207-009-9429-3>
- Wilson OC (1978) Chromospheric variations in main-sequence stars. *ApJ* 226:379–396. <https://doi.org/10.1086/156618>
- Yeo KL, Krivova NA, Solanki SK, HK G (2014) Reconstruction of total and spectral solar irradiance from 1974 to 2013 based on KPVT, SoHO/MDI, and SDO/HMI observations. *Å* 570:85. <https://doi.org/10.1051/0004-6361/201423628>

**Publisher's Note** Springer Nature remains neutral with regard to jurisdictional claims in published maps and institutional affiliations.